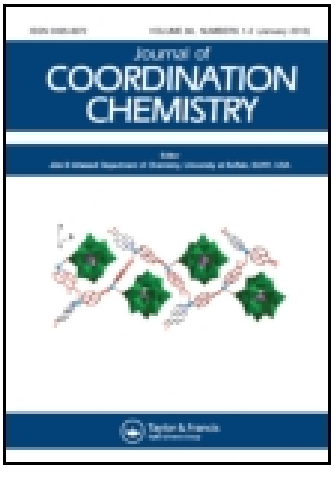

Journal of Coordination Chemistry
Publication details, including instructions for authors and subscription information:
http://www.tandfonline.com/loi/gcoo20

Synthesis and crystal structures of sterically tuned ether functionalized NHC-silver(I) complexes: antibacterial and nucleic acid interaction studies

Rosenani A. Haque[a], Patrick O. Asekunowo[a] & Mohd. R. Razali[a]
[a] The School of Chemical Sciences, Universiti Sains Malaysia, Penang, Malaysia

Accepted author version posted online: 05 Jun 2014.Published online: 02 Jul 2014.

To cite this article: Rosenani A. Haque, Patrick O. Asekunowo & Mohd. R. Razali (2014) Synthesis and crystal structures of sterically tuned ether functionalized NHC-silver(I) complexes: antibacterial and nucleic acid interaction studies, Journal of Coordination Chemistry, 67:12, 2131-2147, DOI: 10.1080/00958972.2014.931575

To link to this article: http://dx.doi.org/10.1080/00958972.2014.931575

Journal of Coordination Chemistry, 2014
Vol. 67, No. 12, 2131–2147, http://dx.doi.org/10.1080/00958972.2014.931575

Synthesis and crystal structures of sterically tuned ether functionalized NHC–silver(I) complexes: antibacterial and nucleic acid interaction studies

ROSENANI A. HAQUE*, PATRICK O. ASEKUNOWO and MOHD. R. RAZALI

The School of Chemical Sciences, Universiti Sains Malaysia, Penang, Malaysia

(*Received 2 January 2014; accepted 23 April 2014*)

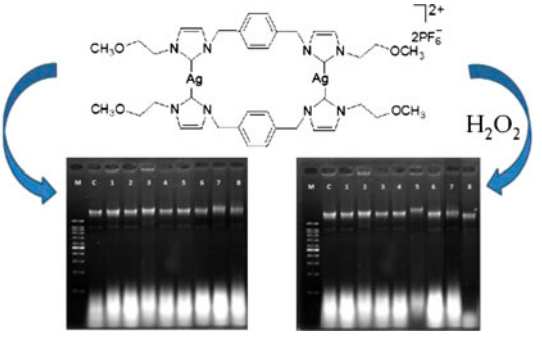

A series of new imidazolium salts (**1–4**) as *N*-heterocyclic carbene (NHC) precursors have been synthesized by successive N-alkylation method. Reactions of these salts with Ag_2O by varying the metal to salt ratio forms a series of new Ag(I)–NHC complexes (**5–8**). All compounds were characterized by physico-chemical and spectroscopic techniques. The molecular structures of **1** and **5** were characterized by single-crystal X-ray diffraction analysis. A comparative investigation of the bacterial growth inhibition potential of the salts and respective complexes indicates that **5–8** displayed good antibacterial activities on *Staphylococcus aureus* (ATCC 12600) and *Escherichia coli* (ATCC 11303) compared with the salts. Furthermore, it was observed that with increase in chain length at *N*-positions, the antibacterial activities also increased. Nuclease activity of the reported salts and Ag(I)–NHC complexes with nucleic acids (DNA and RNA) were also studied using agarose gel electrophoresis; the results show that the compounds do not have any apparent interaction with nucleic acids in the absence of hydrogen peroxide (H_2O_2). However, **5** and **8** were efficient in promoting the cleavage of nucleic acids in the presence of H_2O_2.

Keywords: Ag(I)–NHC complexes; Antibacterial activity; DNA cleavage; *N*-heterocyclic carbene; X-ray diffraction

*Corresponding author. Email: rosenani@usm.my

1. Introduction

Treatment of infectious diseases is becoming a global problem because of increasing numbers of multi-drug-resistant pathogenic bacteria [1, 2]. This has underscored the need for new antimicrobial compounds that will effectively treat resistant bacteria diseases [3, 4]. Silver has been known as a potent antimicrobial agent for centuries [5]. Silver salts are employed especially in the treatment of extensive burns, chronic ulcers, and for prevention of conjunctivitis in addition to bacterial infections [6]. Many *N*-heterocyclic carbene (NHC) silver compounds have been synthesized; Youngs and co-workers in 2004 reported the first Ag(1)–NHC complexes possessing antimicrobial activity [7]. The search for more biologically active Ag(I)–NHC complexes led to the synthesis of modified caffeine silver acetate complex [8]. Ghosh and co-workers also synthesized Ag(I)–NHC complexes of 1-benzyl-3-tert-butylimidazolium chloride and tested on analytically important micro-organisms [9]. The Ag(I)–NHC complexes derived from 4,5-dichloroimidazole have been synthesized, having water stability for up to three days and this was attributed to the presence of electron-withdrawing substituents present on the 4th and 5th positions of the imidazole ring [10]. Varieties of functionalized NHC complexes with bidentate chelating NHCs, tripodal NHCs, and pincer-type NHCs have also been investigated [11–15] especially in catalysis, while their antimicrobial properties are less explored. The effectiveness of the antimicrobial properties of Ag(I) complexes may be influenced by the type of ligands that bind to Ag(I) [16]. Type of substituents and chain length of alkyl chain have a significant effect on their antimicrobial properties [17, 18]. Modification of NHCs can be easily achieved by introducing functional groups at the nitrogens of the imidazole ring [11–13], thereby fine-tuning features like lipophilicity, charge, and solubility of the spacers (bridging groups) and substituents. This has stimulated the design of complexes, reaching a compromise between biological activity and toxic effects [19]. A very interesting characteristic of NHC chemistry is the ease with which a number of complexes with similar structures and different lipophilicity can be prepared by changing the substituents on the imidazolium salts [20, 21]. The lipophilicity of a substance is an influential parameter in biological activity [11–13]. Increased lipophilicity of some compounds has been found to have positive correlation with their antibacterial activity [22, 23]. Also found low viscosity of a compound showed a higher antimicrobial activity [24, 25] and ether group with a lipophilic property and electron-donating ability into cations can help to reduce viscosities, melting point, and reducing degradation, thus retaining the antibacterial effect over a longer period of time [26, 27]. In view of the above observations, the antibacterial and nuclease activities of ether functionalized imidazolium salts and their respective Ag(I)–NHC complexes are hereby investigated.

2. Experimental

2.1. *Materials and measurements*

All chemicals were reagent grade and used as received. NMR spectra were recorded on a Bruker 500 MHz spectrometer at RT in DMSO-d_6, using TMS as an internal standard. FTIR spectra were recorded on a Perkin Elmer-2000 spectrometer from 4000 to 400 cm^{-1}. Elemental analyses were carried out on a Perkin-Elmer series II, 2400 microanalyzer. Melting points were measured using a Stuart Scientific SMP-1 (UK) instrument. The instruments

are available at The School of Chemical Sciences, Universiti Sains Malaysia. The X-ray single-crystal structure analysis was obtained using a Bruker Smart ApexII-2009 CCD area detector diffractometer.

2.2. *Synthesis of 1,4-bis(3-methoxyethylimidazol-1-ylmethyl)benzene hexafluorophosphate (1)*

A mixture of imidazole (2.00 g, 29.38 mM) and KOH (2.47 g, 44.03 mM) in DMSO (30 mL) was stirred for 1 h at RT. 1-Bromo-2-methoxyethane (4.08 g, 29.38 mM) was then added dropwise to the reaction mixture. After 2 h, the mixture was poured into 200–300 mL of water and extracted with chloroform (3 × 30 mL). The extract was filtered twice through four plies of Whatman filter papers in order to dry the extract. The process of filtration was repeated thrice to collect a clear solution of the desired compound, and the solvent was removed under reduced pressure to obtain thick colorless oil. The compound formed, N-methoxyethyl imidazole (0.5 g, 3.97 mM) was added dropwise in a stirring solution of 1,4-bis(bromomethyl)benzene (0.52 g, 1.98 mM) in acetonitrile (30 mL) and then refluxed for 24 h. The solvent was removed under reduced pressure to give 1,4-bis(N-methoxyethylimidazol-1-ylmethyl)benzene dibromide which was then reacted with a solution of KPF_6 (0.73 g, 3.97 mM) in methanol (20 mL). The mixture was stirred at RT for 3 h and allowed to stand overnight. Then, the solvent was removed under reduced pressure and the resultant white powder was washed with distilled water (3 × 10 mL) to remove unreacted KPF_6 and air-dried. The powder was recrystallized in a solution of acetonitrile/methanol to obtain colorless crystals. Yield: 0.8 g (63%). M.p. 168–170 °C; ^{1}H NMR (500 MHz, DMSO-d_6, 298 K, δ ppm): 3.28 (s, 6H, OCH_3); 3.70 (t, J = 5.0 Hz, 4H, **CH_2**–OCH_3); 4.37 (t, J = 5.0 Hz, 4H, 2 × N–CH_2); 5.46 (s, 4H, 2 × N–CH_2–Benzylic); 7.48 (s, 4H, Ar–H); 7.75 (s, 4H, 2 × imidazolium H4′, H5′); 9.27 (s, 2H, 2 × imidazolium H2′); ^{13}C {^{1}H} NMR (125 MHz, DMSO-d_6, 298 K, δ ppm): 49.0 (N–CH_2), 51.5 (CH_2), 58.0 (CH_3), 69.4 (CO), 122.3 (imidazolium C5′), 123.2 (imidazolium C4′), 128.8, 135.4 (Ar–C), 136.5 (imidazolium C2′). FTIR (KBr disk) cm^{-1}: 3405 (C_{aliph}–$N_{imidazole}$), 3128 (C–H_{arom}), 2960 (C–H_{aliph}), 1127 (C_{arom}–$N_{imidazole}$), 1357, 1165 cm^{-1} (C–O–C, C–O). Anal. Calcd for $C_{20}H_{28}N_4F_{12}O_2P_2$: C, 37.2; H, 4.3; N, 8.1. Found: C, 37.3; H, 4.5; N, 8.3.

2.3. *Synthesis of 1-methoxylethyl-3-propylimidazolium hexafluorophosphate (2)*

A mixture of imidazole (1.70 g, 25.00 mM) and KOH (1.96 g, 35.00 mM) in DMSO (30 mL) was stirred for 1 h at room temperature. 1-Bromo-2-methoxyethane (3.48 g, 25.00 mM) was added dropwise to the reaction mixture. After 2 h, the mixture was poured into 200–300 mL of water and extracted with chloroform (3 × 30 mL). The extract was filtered thrice through four plies of Whatman filter papers in order to dry the extract. The process of filtration was repeated thrice to collect clear solution of the desired filtrate, and the solvent was removed under reduced pressure to obtain thick colorless oil. The compound formed, N-methoxyethyl imidazole (0.90 g, 7.14 mM) was added dropwise in a stirring solution of 1-bromopropane (0.88 g, 7.14 mM) in acetonitrile (30 mL) and refluxed for 20 h. The solvent was removed under reduced pressure to give 1-methoxylethyl-3-propylimidazolium dibromide which was then reacted with a solution of KPF_6 (0.60 g, 3.26 mM) in methanol (20 mL). The mixture was stirred at room temperature for 3 h and allowed to stand overnight. Then the solvent was removed under reduced pressure and the resultant white powder was washed with distilled water (3 × 5 mL) to remove unreacted KPF_6, and

air-dried. The powder was purified by acetonitrile/dichloromethane and obtained as white solid. Yield: 1.7 g (78%). M.p. 115–117 °C; ^{1}H NMR (500 MHz, DMSO-d_6, 298 K, δ ppm): 0.80 (t, J = 7.5 Hz, 3H, CH_3), 1.78 (m, 2H, –**CH_2**–CH_3), 3.22 (s, 3H, OCH_3), 3.68 (t, J = 5.0 Hz, 2H, **CH_2**–OCH_3), 4.15 (t, J = 7.0 Hz, 2H, N–**CH_2**–CH_2–CH_3), 4.36 (t, J = 5.0 Hz, 2H, N–**CH_2**–CH_2–OCH_3), 7.71 (s, H, imidazolium H5′), 7.74 (s, H, imidazolium H4′), 9.17 (s, H, imidazolium H2′), ^{13}C {^{1}H} NMR (125 MHz, DMSO-d_6, 298 K, δ ppm): 10.2 (CH_3); 22.8 (**CH_2**–CH_3); 46.3 (OCH_3); 48.6 (**CH_2**–OCH_3); 50.4 (N–**CH_2**–CH_2–CH_3); 57.9 (N–**CH_2**–CH_2–OCH_3); 70.8 (CO); 122.2 (imidazolium C5′); 122.6 (imidazolium C4′); 135.9 (imidazolium C2′). FTIR (KBr disk): 3416 (C_{aliph}–$N_{imidazole}$), 3148 (C–H_{arom}), 2965 (C–H_{aliph}), 1130 (C_{arom}–$N_{imidazole}$), 1355, 1160 cm^{-1} (C–O–C, C–O). Anal. Calcd for $C_9H_{17}N_2OF_6P$: C, 34.4; H, 5.4; N, 8.9. Found: C, 34.6; H, 5.6; N, 9.2.

2.4. *Synthesis of 1-methoxylethyl-3-butylimidazolium hexafluorophosphate (3)*

Salt **3** was prepared in an analogous fashion to **2**, but instead of 1-bromopropane, 1-bromobutane (0.88 g, 7.14 mM) was added. Salt **3** was isolated as a white solid. Yield: 0.8 g (63%). M.p. 120–122 °C. ^{1}H NMR (500 MHz, DMSO-d_6, 298 K, δ ppm): 0.80 (t, J = 7.5 Hz, 3H, CH_3); 1.30 (m, 2H, –**CH_2**–CH_3); 1.78 (m, 2H, N–CH_2–**CH_2**); 3.22 (s, 3H, OCH_3); 3.68 (t, 2H, J = 5.0 Hz, **CH_2**–OCH_3); 4.15 (t, 2H, J = 7.0 Hz, N–**CH_2**–CH_2–CH_3); 4.36 (t, J = 5.0 Hz, 2H, N–**CH_2**–CH_2–OCH_3); 7.71 (s, H, imidazolium H5′); 7.74 (s, H, imidazolium H4′); 9.17 (s, H, imidazolium H2′). ^{13}C {^{1}H} NMR (125 MHz, DMSO-d_6, 298 K, δ ppm): 10.2 (CH_3), 22.8 (**CH_2**–CH_3), 46.3 (OCH_3), 48.6 (**CH_2**–OCH_3), 50.4 (N–**CH_2**–CH_2–CH_3), 57.9 (N–**CH_2**–CH_2–OCH_3), 70.8 (CO), 122.2 (imidazolium C5′), 122.6 (imidazolium C4′), 135.5 (imidazolium C2′). FTIR (KBr disk): 3406 (C_{aliph}–$N_{imidazole}$), 3188 (C–H_{arom}), 2995 (C–H_{aliph}), 1125 (C_{arom}–$N_{imidazole}$), 1307, 1170 cm^{-1} (C–O–C, C–O) cm^{-1}. Anal. Calcd for $C_{10}H_{19}N_2OF_6P$: C, 36.6; H, 5.8; N, 8.5. Found: C, 36.9; H, 6.0; N, 8.8.

2.5. *Synthesis of 1-methoxylethyl-3-pentylimidazolium hexafluorophosphate (4)*

Salt **4** was prepared in an analogous fashion to **2** but instead of 1-bromopropane, 1-bromopentane (0.97 g, 6.40 mM) was added. Salt **4** was isolated as a white solid. Yield: 0.85 g (65%). M.p. 125–127 °C. ^{1}H NMR (500 MHz, DMSO-d_6, 298 K, δ ppm): 0.90 (t, J = 7.5 Hz, 3H, CH_3); 1.25 (m, 2H, –**CH_2**–CH_3); 1.35 (m, 2H, –**CH_2**–CH_2–CH_3); 1.85 (m, 2H, N–CH_2–**CH_2**); 3.30 (s, 3H, OCH_3), 3.80 (t, J = 5.0 Hz, 2H, **CH_2**–OCH_3), 4.25 (t, J = 7.0 Hz, 2H, N–**CH_2**), 4.45 (t, J = 5.0 Hz, 2H, N–**CH_2**–CH_2–OCH_3), 7.85 (s, H, imidazolium H5′), 7.90 (s, H, imidazolium H4′), 9.37 (s, H, imidazolium H2′), ^{13}C {^{1}H} NMR (125 MHz, DMSO-d_6, 298 K, δ ppm): 10.2 (CH_3), 22.8 (**CH_2**–CH_3), 46.3 (OCH_3), 48.6 (**CH_2**–OCH_3), 50.4 (N–**CH_2**–CH_2–CH_3), 57.9 (N–**CH_2**–CH_2–OCH_3), 70.8 (CO), 122.2 (imidazolium C5′), 122.6 (imidazolium C4′), 135.9 (imidazolium C2′), FTIR (KBr disk): 3416 (C_{aliph}–$N_{imidazole}$), 3178 (C–H_{arom}), 2999 (C–H_{aliph}), 1129 (C_{arom}–$N_{imidazole}$), 1327, 1170 cm^{-1} (C–O–C, C–O). Anal. Calcd for $C_{11}H_{21}N_2OF_6P$: C, 40.5; H, 6.4; N, 8.6. Found: C, 40.8; H, 6.7; N, 8.9.

2.6. *Synthesis of 1,4-bis(3-methoxyethylimidazol-1-ylmethyl)benzenesilver(I) bis (hexafluorophosphate) (5)*

Ag_2O (0.35 g, 1.5 mM) was added to a solution of **1** (0.48 g, 0.75 mM) in acetonitrile (35 mL) and the mixture was kept stirring at 50–60 °C for 18 h, covered from light. The mixture

was then filtered through a pad of Celite and the resulting colorless solution was evaporated to give a white solid which was redissolved in acetonitrile, followed by reduction of solvent to about 3 mL. Addition of diethyl ether reprecipitated **5** as a white solid. Yield: 0.5 g (56%). Single crystals of **5** suitable for X-ray were obtained by slow diffusion of diethyl ether into acetonitrile solution containing the complex. M.p. 216–218 °C; ^{1}H NMR (500 MHz, DMSO-d_6, 298 K, δ ppm): 3.17 (s, 12H, 4 × OCH_3); 3.69 (t, J = 5.5 Hz, 8H, 4 × **CH_2**–OCH_3); 4.35 (t, J = 5.0 Hz, 8H, 4 × N–CH_2); 5.31 (s, 8H, 4 × N–CH_2–Benzylic); 7.15 (s, 8H, Ar–H); 7.49 (s, 4H, 2 × imidazolium H5′); 7.55 (s, 4H, 2 × imidazolium H4′); ^{13}C {^{1}H} NMR (125 MHz, DMSO-d_6, 298 K, δ ppm): 50.8 (N–CH_2), 53.6 (CH_2); 58.1 (CH_3); 71.4 (CO); 122.1 (imidazolium C5′); 122.8 (imidazolium C4′); 127.6, 137.1 (Ar–C); 179.9 (imidazolium C2′–Ag). FTIR (KBr disk) cm^{-1}: 3440 (C_{aliph}–$N_{imidazole}$), 3198 (C–H_{arom}), 2985 (C–H_{aliph}), 1327 (C_{arom}–$N_{imidazole}$), 1357, 1165 cm^{-1} (C–O–C, C–O). Anal. Calcd for $C_{40}H_{52}N_8Ag_2O_4F_{12}P_2$: C, 39.5; H, 4.3; N, 9.2. Found: C, 39.7; H, 4.4; N, 9.3.

2.7. *Synthesis of 1-methoxylethyl-3-propylimidazoliumsilver(I) hexafluorophosphate (6)*

Ag_2O (0.37 g, 1.60 mM) was added to a solution of **2** (0.5 g, 1.60 mM) in acetonitrile (35 mL) and the mixture was stirred at 50–60 °C for 12 h, covered from light. The mixture was then filtered through Celite and the resulting colorless solution was evaporated to give a white solid which was redissolved in acetonitrile, followed by reduction of solvent to about 3 mL. Addition of diethyl ether re-precipitated the product as white solid. Single crystals of **6** suitable for X-ray were obtained by ether diffusion. Yield: 0.85 g (88%). M.p. 172–174 °C; ^{1}H NMR (500 MHz, DMSO-d_6, 298 K, δ ppm): 0.88 (t, J = 7.5 Hz, 6H, 2 × CH_3); 1.82 (m, 4H, 2 × –**CH_2**–CH_3); 3.25 (s, 6H, 2 × OCH_3); 3.69 (t, J = 5.0 Hz, 4H, 2 × **CH_2**–OCH_3); 4.11 (t, J = 7.0 Hz, 4H, 2 × N–**CH_2**–CH_2–CH_3); 4.32 (t, J = 5.0 Hz, 4H, 2 × N–**CH_2**–CH_2–OCH_3); 7.48 (s, H, imidazolium H5′); 7.50 (s, H, imidazolium H4′). ^{13}C {^{1}H} NMR (125 MHz, DMSO-d_6, 298 K, δ ppm): 10.8 (CH_3), 24.5 (**CH_2**–CH_3), 46.3 (OCH_3), 50.7 (**CH_2**–OCH_3), 52.5 (N–**CH_2**–CH_2–CH_3), 58.1 (N–**CH_2**–CH_2–OCH_3); 71.4 (CO), 121.7 (imidazolium C5′); 122.2 (imidazolium C4′); 179.3 (imidazolium Ag–C2′). FT-IR (KBr disk) cm^{-1}: 3458 (C_{aliph}–$N_{imidazole}$), 3187 (C–H_{arom}), 2995 (C–H_{aliph}), 1336 (C_{arom}–$N_{imidazole}$), 1355, 1160 cm^{-1} (C–O–C, C–O). Anal. Calcd for $C_{18}H_{32}N_4AgO_2F_6P$: C, 36.7; H, 5.4; N, 9.5. Found: C, 36.8; H, 5.5; N, 9.7.

2.8. *Synthesis of 1-methoxylethyl-3-butylimidazoliumsilver(I) hexafluorophosphate (7)*

Complex **7** was prepared in an analogous fashion to **6** except that **2** was replaced with **3** (1.00 g, 3.20 mM) and Ag_2O (0.72 g, 3.20 mM). Yield: 0.95 g (53%). Single crystals suitable for X-ray were obtained by slow diffusion of diethyl ether into acetonitrile solution containing the complex. M.p. 178–180 °C; ^{1}H NMR (500 MHz, DMSO-d_6, 298 K, δ ppm): 0.88 (t, J = 7.5 Hz, 6H, 2 × CH_3); 1.30 (m, 4H, 2 × –**CH_2**–CH_3); 1.82 (m, 4H, 2 × N–CH_2–**CH_2**); 3.25 (s, 6H, 2 × OCH_3); 3.69 (t, J = 5.0 Hz, 4H, 2 × **CH_2**–OCH_3); 4.11 (t, J = 7.0 Hz, 4H, 2 × N–**CH_2**–CH_2–CH_3); 4.32 (t, J = 5.0 Hz, 4H, 2 × N–**CH_2**–CH_2–OCH_3); 7.48 (s, H, imidazolium H5′); 7.50 (s, H, imidazolium H4′); ^{13}C {^{1}H} NMR (125 MHz, DMSO-d_6, 298 K, δ ppm): δ 10.8 (CH_3); 24.5 (**CH_2**–CH_3); 46.3 (OCH_3); 50.7 (**CH_2**–OCH_3); 52.5 (N–**CH_2**–CH_2–CH_3); 58.1 (N–**CH_2**–CH_2–OCH_3); 71.4 (CO); 121.7 (imidazolium C5′); 122.2 (imidazolium C4′); 177.97 & 179.56 [(d, ^1J(C-^{109}Ag) = 198.5 Hz and d, ^1J(C–^{107}Ag) = 185.0 Hz]. 3406 (C_{aliph}–$N_{imidazole}$); 3188 (C–H_{arom}); 2995

($C–H_{aliph}$); 1275 ($C_{arom}–N_{imidazole}$); 1307, 1170 cm^{-1} (C–O–C, C–O). Anal. Calcd for $C_{20}H_{36}N_4AgO_2F_6P$: C, 38.8; H, 5.8; N, 9.1. Found: C, 39.0; H, 6.0; N, 9.2.

2.9. *Synthesis of 1-methoxylethyl-3-pentylimidazoliumsilver(I) hexafluorophosphate (8)*

Complex **8** was prepared according to the same procedure for **7** except that **2** was replaced with **4** (0.80 g, 2.90 mM) and AgO_2 (0.67 g, 2.90 mM). White solid. Yield: 0.55 g (51%). M.p. 184–186 °C. ^{1}H NMR (500 MHz, DMSO-d_6, 298 K, δ ppm): 0.90 (t, J = 7.5 Hz, 6H, 2 × CH_3); 1.25 (m, 4H, 2 × –**CH_2**–CH_3); 1.35 (m, 4H, 2 × –**CH_2**–CH_3) 1.85 (m, 4H, 2 × CH_2–**CH_2**); 3.30 (s, 6H, 2 × OCH_3), 4.15 (t, J = 5.0 Hz, 4H, 2 × **CH_2**–OCH_3); 4.30 (t, J = 7.0 Hz, 4H, 2 × N–**CH_2**–CH_2–CH_3); 4.72 (t, J = 5.0 Hz, 4H, 2 × N–**CH_2**–CH_2–OCH_3); 7.90 (s, H, imidazolium H5′); 7.95 (s, H, imidazolium H4′). ^{13}C {^{1}H} NMR (125 MHz, DMSO-d_6, 298 K, δ ppm): 10.2 (CH_3); 22.8 (**CH_2**–CH_3); 46.3 (OCH_3); 48.6 (**CH_2**–OCH_3); 50.4 (N–**CH_2**–CH_2–CH_3); 57.9 (N–**CH_2**–CH_2–OCH_3) 70.8 (CO), 122.2 (imidazolium C5′), 122.6 (imidazolium C4′), 180.0 (imidazolium Ag–C2′). FTIR (KBr disk): 3456 ($C_{aliph}–N_{imidazole}$), 3198 ($C–H_{arom}$), 2999 ($C–H_{aliph}$), 1349 ($C_{arom}–N_{imidazole}$), 1327, 1170 cm^{-1} (C–O–C, C–O). Anal. Calcd for $C_{20}H_{36}N_4AgO_2F_6P$: C, 38.9; H, 5.8; N, 9.1. Found: C, 40.3; H, 6.1; N, 9.3.

2.10. *Antibacterial studies*

Stock solutions of all compounds were prepared using DMSO. Antibacterial tests were performed using the Kirby Beur disk diffusion method [28]. Single colonies of *Escherichia coli* (ATCC 11303) and *Staphylococcus aureus* (ATCC 12600) from fresh culture agar plates were, respectively, cultured in two bottles containing 5 mL nutrient broth solution and incubated overnight at 37 °C. The turbidity of each culture was adjusted by comparing it to 0.5 McFarland standard, which is equal to 1.58×10^8 CFU mL^{-1} or 0.5 ($O.D_{600}$ reading). Using sterile cotton buds, each bacterial lawn culture was spread uniformly on different agar plates before placing the antimicrobial assay disks on the plate. Four disks were placed on each agar plate and 5 µL volumes of the test compounds were loaded on the disks with concentrations at 100 and 50 µg mL^{-1}. The plates were incubated at 37 °C for 24 h and the diameters of inhibition zones were measured in mm. The antibacterial test was calculated as the mean of three replicates. The effectiveness of these compounds in relation to inhibition zone was compared with silver nitrate, based on its established antimicrobial properties [29] and streptomycin was used as positive control. The minimum inhibitory concentration (MIC) of each compound was determined based on the lowest concentration of the compound that inhibited the growth of bacteria using the broth dilution method [30]. Single colonies of *S. aureus* and *E. coli* were isolated from agar plates and were grown in 5.0 mL LB broth. The solutions were incubated at 37 °C and shaken at 180 rpm overnight to yield bacteria solutions. Stock solutions of the compounds were prepared by dissolving each in DMSO to give stock concentrations of 50 mg mL^{-1}. Respectively from each stock solution, 2 µL of the compounds (salts and complexes), $AgNO_3$, and streptomycin were dissolved in 2 mL of the broth culture and used to prepare four serial dilutions of 100, 50, 25, and 12.5 µg mL^{-1}. Serial dilutions were done for each compound by transferring 1 mL (100 µg mL^{-1}) of the compound solution from the first tube to the second tube already containing 1 mL of nutrient broth. Next, 1 mL from tube 2 was again transferred into tube 3 and another 1 mL from tube 4 to give the concentration of 50, 25, and 12.5 µg mL^{-1},

respectively. Prepared bacteria solution (5 μL) was added to each tube, and the tubes were incubated at 37 °C for 16 h in a shaking incubator at 180 rpm. Bacterial growth was noted by the turbidity of the solution in the tubes and MIC was determined by the lowest concentration lacking turbidity.

2.11. *Gel electrophoresis*

The electrophoresis method was employed to study the interaction of the test compounds with nucleic acids [31]. The extracted plasmid DNA and RNA, pTS414 (10 μg mL^{-1}), and 1 μL of the test sample (50 μg mL^{-1}) were mixed in 50 mM Tris-HCl buffer (pH 8.00). The contents were incubated for 8 h at 37 °C. Plasmid extraction was done using a plasmid purification kit (Intron Biotechnology, Korea) without the addition of RNase in order to extract both RNA and DNA. The electrophoresis was performed using 0.8% Agarose gel. For each sample, 5 μL of the mixture was loaded into the well. The voltage used was 90 V running on 0.5 × Tris-Acetate EDTA (TAE) buffer and the gel was stained with ethidium bromide solution (10 μg mL^{-1}) for 15 min. The gel was subsequently exposed to UV light and captured by a gel documentation system (FluorChem HD2; Cell Bioscience). The nucleating abilities of the synthesized imidazolium salts/Ag–NHC complexes (**1–8**) were determined by its efficiency in cleaving/degrading the plasmid DNA and RNA. The same procedure was used in the presence of H_2O_2 oxidant.

3. Results and discussion

3.1. *Synthesis and characterization*

The NHC precursors (**1–4**) were synthesized from reactions between bis(bromomethyl)benzene, 1-bromopropane, 1-bromobutane, 1-bromopentane, and N-methoxyethylimidazole in refluxing acetonitrile for 20–24 h to yield the desired products **1–4**, respectively. The obtained bromide salts were converted to hexafluorophosphate salts (in order to enhance their solubility, stability and easier handling) by metathesis with KPF_6 in methanol to obtain **1–4** as a white solid in moderate yield. Elemental analyses of the salts agree with the proposed composition and their ^{1}H NMR spectra showed the expected signals for the imidazolium salts. Complex **5** was prepared in 1 : 2 M ratio of **1** to Ag_2O, while **6–8** were prepared in equimolar reactions of **2–4** with Ag_2O in acetonitrile at 50–60 °C for 12–18 h, covered from light. All the NHC complexes (**5–8**) were purified by repeated precipitation in acetonitrile by the addition of diethyl ether. The complexes are soluble in acetonitrile, acetone, and DMSO but are insoluble in water, ethyl acetate, hexane, diethyl ether, and toluene. The synthetic route to the formation of NHC precursors (**1–4**) and their respective Ag(I)–NHC complexes (**5–8**) are outlined in schemes 1 and 2.

3.2. *Hydrolysis test*

Solution studies of these complexes were essential in order to identify the bioactive species resulting from dissolution of the solid complex, and so understand the underlying biochemical mechanism involved in the antibacterial activity. This study is also relevant to the antibacterial studies since the complexes have to be maintained in culture medium for at least

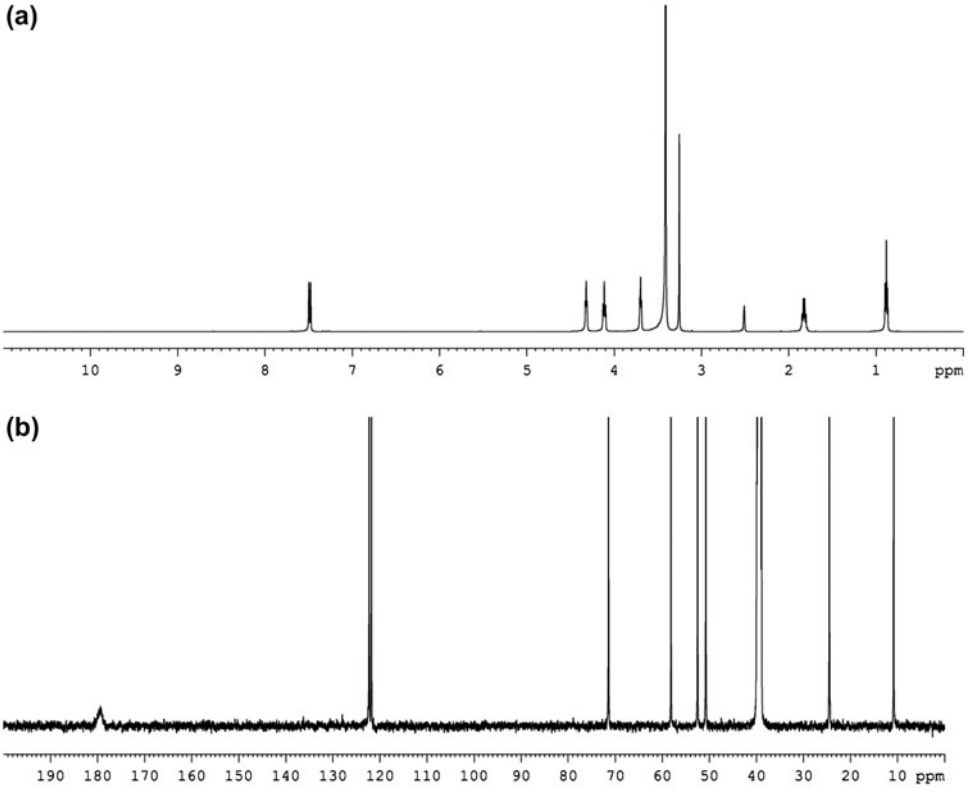

Figure 1. Representative (a) ^{1}H NMR and (b) ^{13}C NMR spectra of **6** after 48 h in 10% aqueous DMSO.

24 h. Therefore, we have determined the stabilities of the Ag–NHC complexes **5–8** in both 10 and 100% DMSO-d_6 aqueous solution. Both complexes are stable in aqueous solution for 48 h, since their ^{1}H NMR spectra remained unchanged after 48 h. The representative ^{1}H and ^{13}C NMR spectra of **6** after 48 h in 10% aqueous DMSO is shown in figure 1 and is identical to the spectra obtained after 15 min (see supplementary data figure S8, http://dx.doi.org/10.1080/00958972.2014.931575).

In order to further assess the stability of the complexes in the broth mixture, 10 mg mL^{-1} stock solutions of the complexes in DMSO were prepared and added in a 1 : 1 ratio to LB broth prepared in DMSO. This was done to imitate the conditions of the MIC evaluation experiments. The ^{1}H NMR and ^{13}C NMR spectra were taken after 15 min and 24 h. The complexes demonstrated stability in the LB/DMSO broth mixture at 37 °C, as shown by the unchanged ^{1}H and ^{13}C NMR spectra after 24 h. However, the circumstances under physiological conditions may vary, but these preliminary results are noteworthy.

3.3. *FTIR spectra*

FTIR data can be used as a preliminary confirmation for synthesis of Ag(I)–NHC complexes because they usually show some characteristic peaks comparable to the respective proligands [32]. For all analyzed salts, sharp stretching vibrations were observed at 1170–1357 cm^{-1} ascribed to the C–O and C–O–C modules and remained unchanged in the

spectra of Ag(I)–NHC complex. This suggests the presence of ether functionality outside the coordination sphere (oxygen functionalities are not coordinated), which is further confirmed by X-ray diffraction analysis. The NHC carbon, upon complexation with silver, alters the vibration bands. This is evident at 1125–1130 cm^{-1} for the salts and 1275–1349 cm^{-1} for the Ag(I)–NHC complexes, assignable to imidazole ring $\nu(C_{arom}–N_{imidazole})$ vibrations [33] and this pattern appears for all the complexes. However, metal-to-carbene carbon vibrations are normally observed in far-IR region and, therefore, could not be assigned in the available IR spectral data.

3.4. *NMR spectra*

The ^{1}H NMR spectra of imidazolium salts **1–4** in DMSO-d_6 exhibit a characteristic NCHN proton resonance at ca. 9.17–9.37 ppm, suggesting formation of the desired salts. Two doublets at ca. 7.8 ppm were observed for imidazolium C4H and C5H resonances, respectively. Further, methoxy protons and ethylene protons of ether-functionality resonated as a singlet and two triplets in the range ca. 3.22–3.28 and 3.68–4.37 ppm, respectively. Finally, alkyl proton resonances were found in the range ca. 0.8–4.4 ppm, which is in agreement with the similar structures [34]. The ^{13}C NMR spectra of the salts displayed prominent peaks in the downfield region at ca. 135.94–136.51 ppm, attributed to imadazole ring carbene carbon [35–37]. The signals for benzylic (N–CH_2–benzylic) and alkyl chain (–CH_2–) were observed at ca. 51.22–52.27 and 10.00–49.87 ppm, respectively. As expected, in the ^{1}H NMR spectra, the peak corresponding to the NCHN proton resonance completely disappeared, suggesting complex formation which is further confirmed by the downfield shift of carbene carbon nuclei to ca. 179–180 ppm in the ^{13}C NMR spectra. Surprisingly, for **7**, ^{13}C NMR spectrum displayed a downfield resonance for the C2-carbon nuclei as two doublets centered at 178 and 180 ppm. This is due to the presence of ^{13}C–^{109}Ag and ^{13}C–^{107}Ag with the coupling constants of ^1J(C–^{109}Ag) 198.5 and ^1J(C–^{107}Ag) 185.0 Hz, respectively. This observation is in accord with the similar reported compounds [34, 38]. Apart from these major changes, there are no observable changes observed in both spectra.

Table 1. Crystal data and structure refinement details for **1** and **5**.

Formula	$C_{20}H_{28}N_4F_{12}O_2P_2$	$C_{40}H_{52}N_8Ag_2O_4F_{12}P_2$
Formula wt.	646.40	1214.58
Crystal system	Triclinic	Triclinic
Space group	*P–1*	*P–1*
a (Å)	9.0505(2)	11.1859(2)
b (Å)	10.1646(2)	11.5922(2)
c (Å)	15.8288(3)	11.8396(2)
α (°)	81.4000(10)	61.428(1)
β (°)	74.6060(10)	63.427(1)
γ (°)	69.3910(10)	87.524(1)
V (Å^3)	1311.54(5)	1177.61(4)
Z	2	1
ρ (cal g^{-1} cm^{-3})	1.637	1.713
Temperature (K)	100	100
Λ (Mo Kα)	0.71073	0.71073
μ (mm^{-1})	0.279	0.997
Crystal size (mm)	0.50 × 0.38 × 0.22	0.37 × 0.30 × 0.22
R_{int}	0.0230	0.027
$F_{(000)}$	660	612
R_1, wR_2	0.0443, 0.1147	0.0431, 0.1305

3.5. *Single-crystal X-ray diffraction studies*

The crystal data of **1** and **5** are shown in table 1, while the selected bond lengths and angles are given in tables 2 and 3. Compound **1** crystallizes in the triclinic, space group *P−1*, containing one paraxylyl bridged *bis*-carbene cation and two hexafluorophosphate anions in the asymmetric unit (figure 2). The internal ring angles of imidazole (N–C–N) are 108.66(15) for N3–C14–N4 and 108.56(15) for N1–C1–N2, respectively. The central benzene ring (C1–C6) makes dihedral angles of 112.1(1)° and 111.42(2)° with the imidazole rings, (N3–C11–C8) and (N2–C4–C5), respectively, almost perpendicular to the plane of the xylyl group.

Complex **5** crystallizes in the triclinic space group *P−1* with half of the molecule contained in the asymmetric unit. The structure consists of ligands **1**, each of them displays the μ_2-κ^1(C)Ag : κ^1(C′)Ag′ bridging mode, facilitating the formation of dinuclear complex [figure 3(a)]. In this dinuclear complex, each silver ion displays a linear coordination geometry with the Ag1–C1 and Ag1^{i}–C15 distances 2.105(3) and 2.101(3) Å, respectively, while the angle of C1–Ag1–C15^{i} (and its symmetry equivalent) is 177.59(10)°. The Ag–C bond distances for both sets of imidazolium rings at Ag1 and Ag1^{i} are in accord with comparable imidazolium complexes of Ag(I) [39]. The internal ring angles between the planes of the two imidazolin-2-ylidene rings for Ag1 and Ag1^{i} are 123.7(3)°–131.1(3)° and are oriented at the dihedral angles of 12.6(6)°. Each dinuclear complex interdigitates with each other in which the methoxy group is directed into the cavities of the adjacent molecule, facilitating the formation of a 1-D network [figure 3(b)].

3.6. *Antibacterial activity*

Stock solutions of all the compounds were prepared in DMSO. All dilutions were carried out with distilled water. The concentrations of the test compounds were 12.5, 25, 50, and

Table 2. Selected bond lengths (Å) and angles (°) for **1**.

N1–C1	1.331(2)
N2–C1	1.385(2)
N3–C15	1.329(2)
N4–C15	1.333(2)
N1–C1–N2	108.56(15)
N3–C15–N4	108.66(15)

Table 3. Selected bond lengths (Å) and angles (°) of **5**.

Ag1–C1	2.105(3)
N1–C1	1.329(4)
N2–C1	1.368(4)
Ag1^{i}–C15	2.101(3)
N3–C15	1.370(4)
N4–C15	1.321(4)
N1–C1–N2	105.4(3)
N3–C15–N4	105.0(3)
C1–Ag1–C15^{i}	177.59(10)

Note: Symmetry element used: $^{i}1-x, 2-y, -z$.

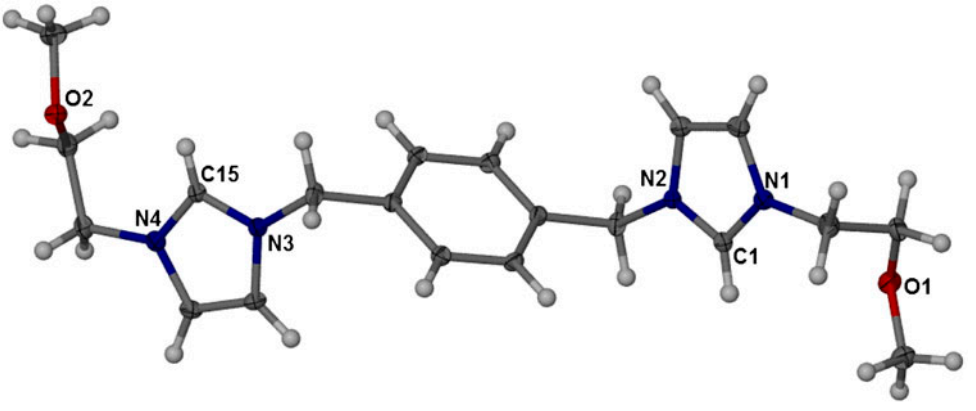

Figure 2. Structure of **1** with the ellipsoids shown at 50% probability. Two hexafluorophosphate anions in the lattice were omitted for clarity.

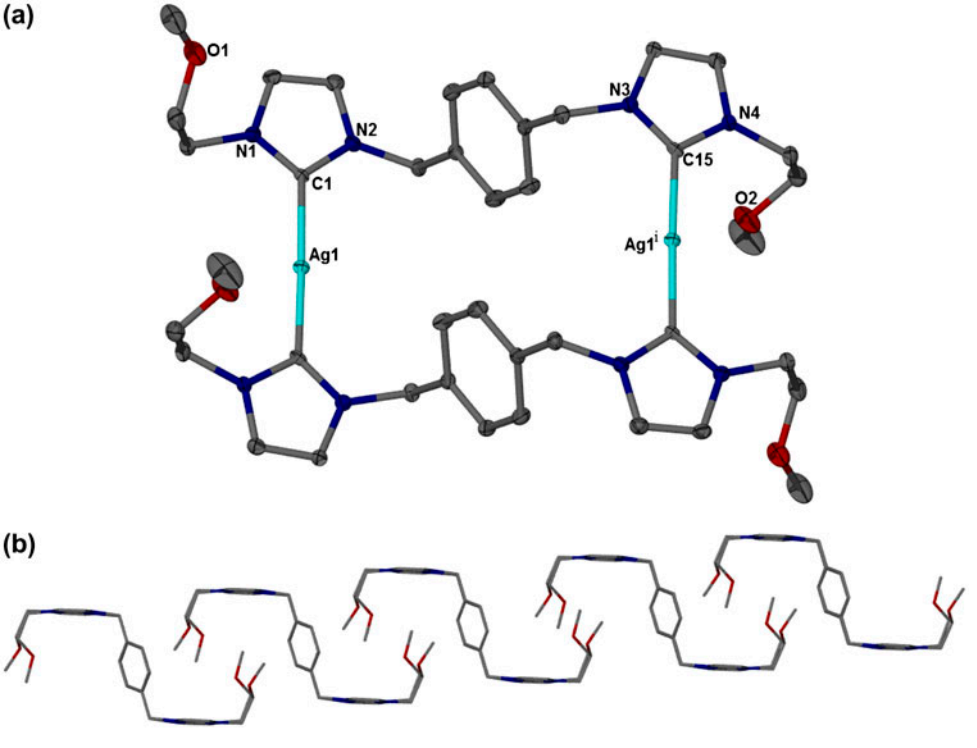

Figure 3. (a) Structure of **5** with ellipsoids shown at 50% probability. Hydrogens and hexafluorophosphate have been omitted for clarity. Symmetry element used: $^{i}1-x, 2-y, -z$. (b) Interdigitate interactions between dinuclear complex in **5**.

100 μg mL^{-1} using silver nitrate for positive control and streptomycin as the standard drug. Compounds were screened for their antibacterial activity against *E. coli* and *S. aureus* using the disk diffusion method. The MIC was determined based on the lowest concentration that

inhibited growth of the bacteria. The antibacterial activities of all complexes showed good inhibition against both the Gram-negative (*E. coli*) and Gram-positive (*S. aureus*) bacteria. However, no inhibition was observed for all salt samples [tables 4(a), 4(b), and figure 4]. From these results, the antibacterial activity of **5** (MIC, 12.5 μg mL^{-1}) was the highest. The MIC values for the complexes against both Gram-positive and Gram-negative bacteria are 12.5–100 μg mL^{-1} (table 5). These values are comparable to the MIC for silver nitrate (50 μg mL^{-1}) and some other related results in the literature [5(b), 40–42], showing that these new Ag–NHC complexes are potent. Salts (**1–4**) do not show any activity. The complexes (**5–8**) showed bacteriostatic activities against both Gram-positive and Gram-negative bacteria, which is in agreement with the literature [43]. Complexes **5** and **8** showed significant bacteriostatic effect against Gram-positive bacteria at 12.5 and 25 μg mL^{-1}, respectively, while for **6**, the activity was 100 μg mL^{-1} (table 5). The present results showed that **5** (dinuclear silver complex) and mononuclear **8**, which is bearing the N-pentyl substituent, are the most sensitive against both Gram-negative and Gram-positive bacteria compared to mononuclear **6** and **7**. This further underscores the existing literature that the number of silver centers within the complex molecule determines their biological activities [44]. It is quite obvious that **8** showed better antibacterial activity (MIC 25 μg mL^{-1}) for the Gram-positive bacteria than **6** and **7** (MIC, 100 and 50 μg mL^{-1}), respectively. Although **6**, **7**, and **8** are mononuclear, they possess different N-alkyl substitution; complex **8** bearing N-pentyl substituent has better antibacterial activity in comparison with others bearing N-propyl and butyl substituents. The order of activity in this work as it relates to chain length seems to be in agreement with previous work carried out by our research group and other researchers, where it was found that the biological activity increased with the increase in chain length for complexes [45–48]. Therefore, the antibacterial activity could be due to lipophilicity of the complexes which may enhance the transport of NHCs into the cell and

Table 4(a). Antibacterial activities of the compounds[a] against *E. coli* and *S. aureus* obtained by the disk diffusion method[b] (zone of inhibition).

	Inhibition zone (mm)					
	Test compound (100 μg mL^{-1})					
Strain	**5**	**6**	**7**	**8**	$AgNO_3$	Streptomycin
E. coli	27 ± 1	10.0 ± 0.7	20 ± 1	24 ± 1	23 ± 3	32.0 ± 0.5
S. aureus	28 ± 1	14.0 ± 0.4	22.0 ± 0.5	28 ± 2	23.7 ± 0.5	32.5 ± 0.5

[a]Compounds **1–4** showed no activity.
[b]Test compound volume = 5 μL; test compound concentrations = 100 μg mL^{-1}.

Table 4(b). Antibacterial activities of the compounds[a] against *E. coli* and *S. aureus* obtained by the disk diffusion method[b] (zone of inhibition).

	Inhibition zone (mm)				
	Test compound (50 μg mL^{-1})				
Strain	**5**	**7**	**8**	$AgNO_3$	Streptomycin
E. coli	20 ± 1	15.0 ± 0.8	18 ± 2	17.0 ± 0.5	23.0 ± 0.5
S. aureus	20.2 ± 0.5	16 ± 3	21.0 ± 0.7	18.5 ± 0.7	23.5 ± 0.5

[a]Compounds **1–4** and **6** showed no activity.
[b]Test compound volume = 5 μL; test compound concentrations = 50 μg mL^{-1}.

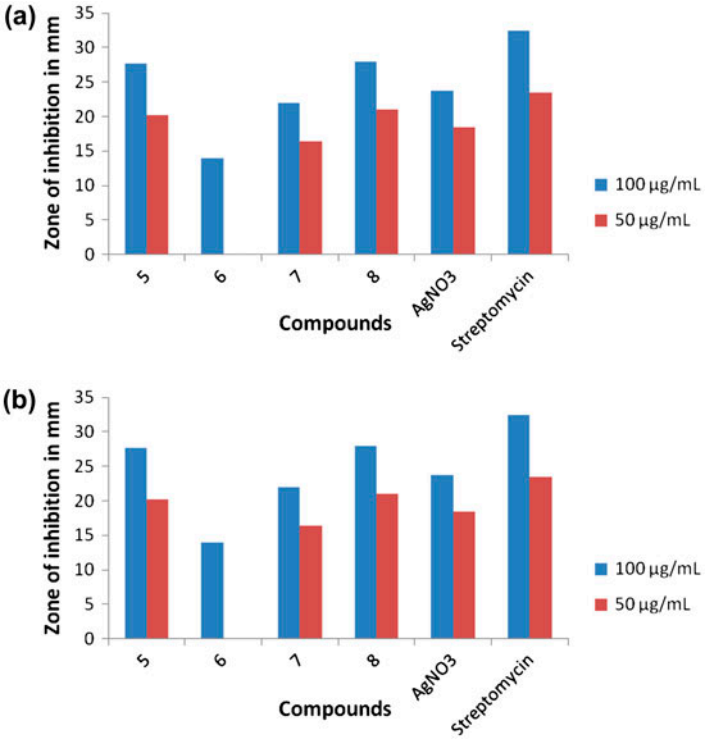

Figure 4. Antimicrobial activity of investigated compounds against (a) *E. coli* and (b) *S. aureus* after being treated with samples solution.

Table 5. MIC against *E. coli* (Gram-negative bacteria) and *S. aureus* (Gram-positive bacteria).

Test compound	*E. coli* ($\mu g\ mL^{-1}$) MIC	*S. aureus* ($\mu g\ mL^{-1}$) MIC
5	25	12.5
6	100	100
7	50	50
8	25	25
$AgNO_3$	50	50
Streptomycin	12.5	12.5

Note: **1–4** did not show activity.

subsequently into the cell organs, where silver may inhibit cellular respiration and metabolism of biomolecules. All the complexes exhibited moderate to good bacteriostatic effect against Gram-negative and Gram-positive bacteria, when compared with streptomycin, while **5** and **8** show better activity than $AgNO_3$ (table 5). However, the NHC precursors showed poor reaction against Gram-positive and Gram-negative bacteria. Such increased activity of the metal complexes relative to their corresponding NHC precursors can be explained on the basis of chelation theory [49].

3.7. *Nuclease activity*

Gel electrophoresis was used to evaluate the nuclease properties of the reported compounds. Plasmid extraction was done using a plasmid purification kit (Intron Biotechnology, Korea) without the addition of RNase in order to extract both RNA and DNA. This method is intended to further investigate the interaction of these synthesized compounds with DNA and/or RNA as a preliminary study for studying likely mode of action(s) of the reported compounds; DNA and also RNA are part of the possible targets of most current bactericidal antimicrobials [50]. Agarose gel image showing the effects of compounds on nucleic acids is shown in figure 5. Compounds **1**–**8** were studied for their interactions with nucleic acids by agarose gel electrophoresis against plasmid, pTS414 DNA/RNA in the presence and absence of H_2O_2 as an oxidizing agent. The electrophoresis analysis showed that the imidazolium salts **1**–**4** displayed no visible activity towards nucleic acids (DNA and RNA) in the presence and absence of H_2O_2 (lanes 1, 2, 3, and 4). Also, there was no observed activity for the complexes in the absence of H_2O_2; however, **5** and **8** displayed activity in the

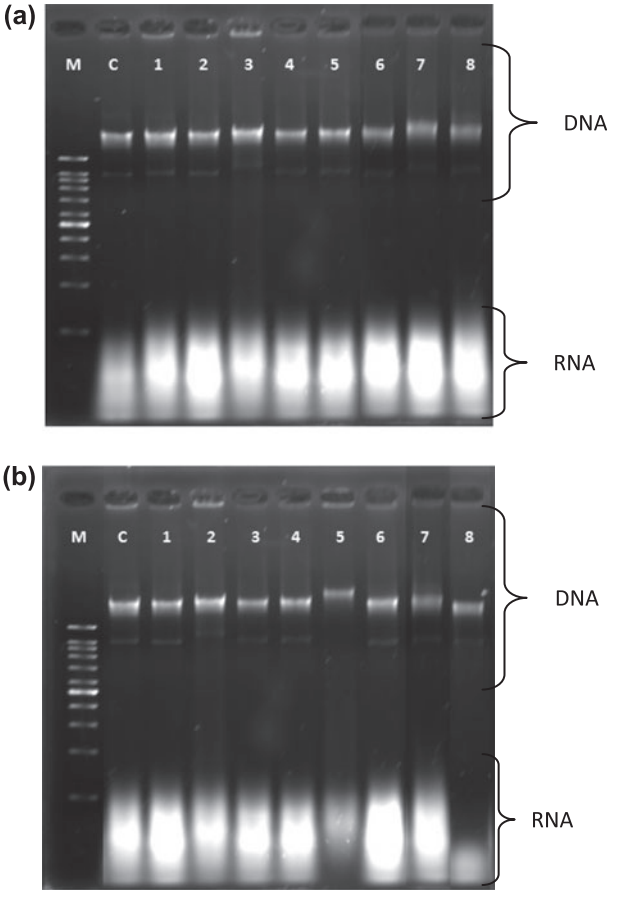

Figure 5. (a) Nuclease activity in the absence of H_2O_2 and (b) in the presence of H_2O_2 at 50 μg mL^{-1}. M: Marker; C: DNA/RNA alone; Lane 1: DNA/RNA + **1**; Lane 2: DNA/RNA + **2**; Lane 3: DNA/RNA + **3**; Lane 4: DNA/RNA + **4**; Lane 5: DNA/RNA + **5**; Lane 6: DNA/RNA + **6**; Lane 7: DNA/RNA + **7**; Lane 8: DNA/RNA + **8**.

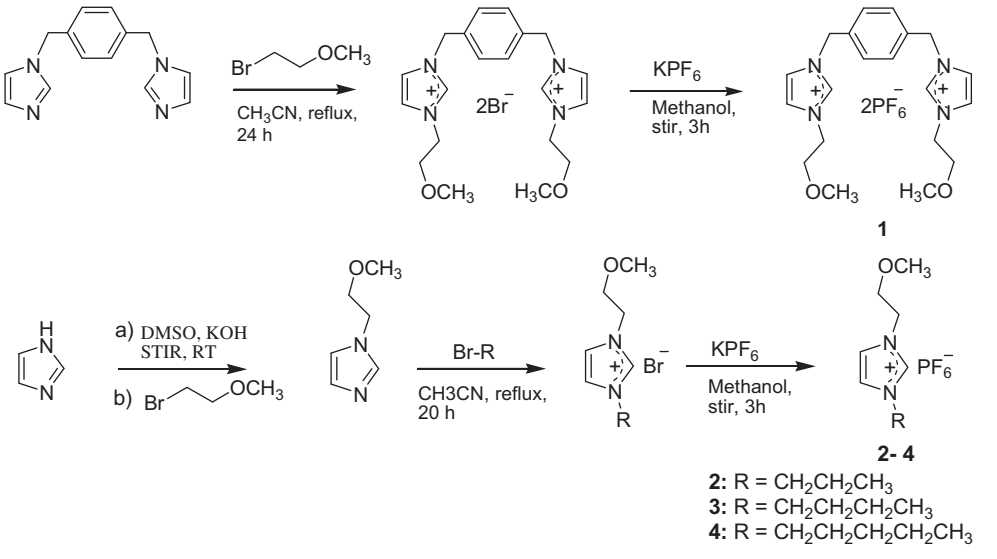

Scheme 1. Synthesis of bis and mono-imidazolium salts (**1–4**).

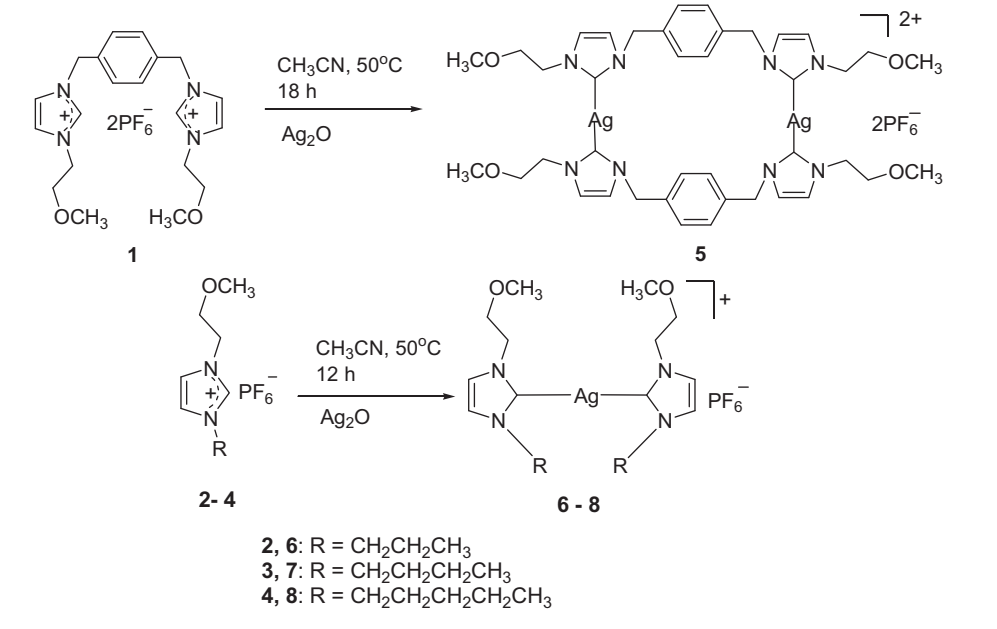

Scheme 2. Synthetic pathway to Ag(I)–mono/bis-NHC complexes (**5–8**) from NHC precursors (**1–4**).

presence of the oxidant; in lane 8 for **8** there was no observed interaction with DNA but the RNA is degraded. There is disappearance of supercoiled DNA strand (absence of the marker band), indicating that **5** displayed complete DNA cleavage and also RNA degradation appearing (lane 5). Possible reaction mechanisms for DNA cleavage in the presence of H_2O_2 have been reported [51, 52]. This study has shown that the control DNA/RNA alone

(lane 2) does not show any apparent cleavage both in the absence and presence of H_2O_2, whereas **5** and **8** do show activity (lanes 5 and 8), respectively. Perhaps **5** and **8** have different pathway of action, as they have shown variation in the activity against DNA and RNA. However, further studies need to be carried out in this respect.

4. Conclusion

We report the synthesis, crystal structures, nucleic acid interaction study, and investigation of antibacterial properties of a new series of NHC precursors (**1–4**) and respective Ag–NHC complexes (**5–8**) in anticipation of discovering new compounds that will serve as antibacterial and nucleic acids cleaving agents. From the antibacterial results, we can conclude that the NHC precursors showed no antibacterial activity when compared with the silver complexes, which have promising results, with good activity against *E. coli* (Gram-negative bacteria) and *S. aureus* (Gram-positive bacteria). The nuclease studies revealed that **5** and **8** possess nuclease activity.

Supplementary material

Crystallographic data for the structure in this work has been deposited at the Cambridge Crystallographic Data Centre, CCDC 941464 and 939882. Copies of these materials can be obtained from the Director, CCDC, 12 Union Road, Cambridge CB2 1EZ, UK (Fax: +44 1223 336033; Email: deposit@ccdc.cam.ac.uk/deposit).

Acknowledgements

The authors thank Universiti Sains Malaysia (USM) for the Research University (RU) [grant number 1001/PKIMIA/811217]. The authors are grateful to Prof. A.A. Amirul of the School of Biological Sciences, Universiti Sains Malaysia for his useful technical assistance.

References

[1] S. Saha, D. Dhanasekaran, S. Chandraleka, N. Thajuddin, A. Panneerselvam. *Adv. Biomed. Res.*, **4**, 224 (2010).
[2] M.E. Mulligan, K. Murray-Leisure. *Am. J. Med.*, **94**, 313 (1993).
[3] R. Bax, R. Bywater, G. Cornaglia. *Clin. Microbiol. Infect.*, **7**, 316 (2001).
[4] D.M. Livermore. *Clin. Microbiol. Infect.*, **10**, 1 (2004).
[5] (a) İ. Özdemir, N. Gürbüz, Ö. Doğan, S. Günal, İ. Özdemir. *Inorg. Chim. Acta*, **24**, 758 (2010); (b) B. Yığıt, Y. Gök, I. Özdemır, S. Günal. *J. Coord. Chem.*, **65**, 371 (2012); (c) Y. Li, X. Dong, Y. Gou, Z. Jiang, H.-L. Zhu. *J. Coord. Chem.*, **64**, 1663 (2011); (d) I. Özdemir, S. Demir, S. Günal, C. Arıcı, D. Ülkü. *Inorg. Chim. Acta*, **363**, 3803 (2010).
[6] T.A. Bell, J.T. Grayston, M.A. Krohn, R.A. Kronmal. *Pediatrics*, **92**, 755 (1993).
[7] A. Melaiye, R.S. Simons, A. Milsted, F. Pingitore, C. Wesdemiotis, C.A. Tessier, W.J. Youngs. *J. Med. Chem.*, **47**, 973 (2004).
[8] A. Kascatan-Nebioglu, A. Melaiye, K. Hindi, S. Durmus, M. Panzner, L. Hogue, R. Mallett, C. Hovis, M. Coughenour, S. Crosby, A. Milsted, D. Ely, C. Tessier, C. Cannon, W.J. Youngs. *J. Med. Chem.*, **49**, 6811 (2006).

[9] S. Ray, R. Mohan, J.K. Singh, M.K. Samantaray, M.M. Shaikh, D. Panda, P.J. Ghosh. *J. Am. Chem. Soc.*, **129**, 15042 (2007).
[10] K. Hindi, T. Siciliano, S. Durmus, M. Panzner, D. Medvetz, D.V. Reddy, L. Hogue, C. Hovis, J. Hilliard, R. Mallet, C. Tessier, C. Cannon, W.J. Youngs. *J. Med. Chem.*, **51**, 1577 (2008).
[11] O. Kühl. *Chem. Soc. Rev.*, **36**, 592 (2007).
[12] A.T. Normand, K.J. Cavell. *Eur. J. Inorg. Chem.*, **14**, 2781 (2008).
[13] A. John, P. Ghosh. *Dalton Trans.*, 7183 (2010).
[14] (a) P.L. Arnold, M. Rodden, K.M. Davis, A.C. Scarisbrick, A.J. Blake, C. Wilson. *Chem. Commun.*, **14**, 1612 (2004); (b) S.T. Liddle, P.L. Arnold. *Chem. Commun.*, **1**, 3559 (2006); (c) D. Pugh, A.A. Danopoulos. *Coord. Chem. Rev.*, **251**, 610 (2007); (d) Y. Zhou, W. Chen. *Organometallics*, **26**, 2742 (2007).
[15] C. Bocchino, M. Napoli, C. Costabile, P. Longo. *J. Polym. Sci., Part A: Polym. Chem.*, **49**, 862 (2011).
[16] K. Nomiya, S. Takahashi, R. Noguchi, S. Nemoto, T. Takayama, M. Oda. *Inorg. Chem.*, **39**, 3301 (2000).
[17] A. Busetti, D.E. Crawford, M.J. Earle, M.A. Gilea, B.F. Gilmore, S.P. Gorman, G. Laverty, A.F. Lowry, M. McLaughlin. *Green Chem.*, **12**, 420 (2010).
[18] J. Pernak, P. Chwała. *Eur. J. Med. Chem.*, **38**, 1035 (2003).
[19] H.T. Chifotides, K.R. Dunbar. *Acc. Chem. Res.*, **38**, 146 (2005).
[20] D. Bourissou, O. Guerret, F.P. Gabbaï, G. Bertrand. *Chem. Rev.*, **100**, 39 (2000).
[21] W.A. Herrmann, C. Köcher. *Angew. Chem. Int. Ed.*, **36**, 2162 (1997).
[22] C.G. de Almeida, G.D. Garbois, L.M. Amaral, C.C. Diniz, M. Le Hyaric. *Biomed. Pharmacother.*, **64**, 287 (2010).
[23] K. Subramani, R. Margabandu. *Int. J. Chem. Tech. Res.*, **2**, 3 (2010).
[24] M. Jumaa, F.H. Furkert, B.W. Müller. *Eur. J. Pharm. Biopharm.*, **53**, 115 (2002).
[25] R. Margabandu, K. Subramani. *Int. J. Chem. Tech. Res.*, **3**, 2 (2010).
[26] S. Fang, Y. Jin, L. Yang, S.I. Hirano, K. Tachibana, S. Katayama. *Electrochim. Acta*, **56**, 4663 (2011).
[27] M.J. Monteiro, F.F. Camilo, M.C.C. Ribeiro, R.M. Torresi. *J. Phys. Chem.*, **114**, 12488 (2010).
[28] W.L. Drew, A.L. Barry, R. O'Toole, J.C. Sherris. *Appl. Microbiol.*, **24**, 240 (1972).
[29] A.B. Lansdown, A. Williams, S. Chandler, S. Benfield. *J. Wound Care*, **14**, 155 (2005).
[30] I. Wiegand, K. Hilpert, R.E.W. Hancock. *Nat. Protoc.*, **3**, 163 (2008).
[31] N. Raman, R. Jeyamurugan, A. Sakthivel, L. Mitu, *Spectrochim. Acta, Part A*, **75**, 88 (2010).
[32] M.A. Iqbal, R.A. Haque, M.B.K. Ahamed, A.M.S. Abdul Majid, S.S. Al-Rawi. *Med. Chem. Res.*, **22**, 2455 (2013).
[33] S. Budagumpi, V.K. Revankar. *Transition Met. Chem.*, **35**, 649 (2010).
[34] R.A. Haque, M.A. Iqbal, S. Budagumpi, M.B.K. Ahamed, A.M.S. Abdul Majid, N. Hasanudin. *Appl. Organomet. Chem.*, **27**, 214 (2013).
[35] F.E. Hahn, M.C. Jahnke, T. Pape. *Organometallics*, **26**, 150 (2007).
[36] F.E. Hahn. *Angew. Chem. Int. Ed.*, **45**, 1348 (2006).
[37] M. Poyatos, J.A. Mata, E. Falomir, R.H. Crabtree, E. Peris. *Organometallics*, **22**, 1110 (2003).
[38] M.V. Baker, D.H. Brown, R.A. Haque, B.W. Skelton, A.H. White. *Dalton Trans.*, 3756 (2004).
[39] *Cambridge Structural Database (Version 5.33)*, The Cambridge Crystallographic Data Centre, Cambridge (2011).
[40] R.A. Haque, P.O. Asekunowo, M.R. Razali. *Transition Met. Chem.*, **39**, 281 (2014).
[41] İ. Özdemir, E.O. Özcan, S. Günal, N. Gürbüz. *Molecules*, **15**, 2499 (2010).
[42] A.R. Knapp, M.J. Panzner, D.A. Medvetz, B.D. Wright, C.A. Tessier, W.J. Youngs. *Inorg. Chim. Acta*, **364**, 125 (2010).
[43] M.O. Agwara, P.T. Ndifon, M.K. Ndikontan, M.A. Atamba. *Res. J. Chem. Environ.*, **12**, 87 (2008).
[44] H. Mahboobi, A. Viarengo, D. Colangelo, D. Osella. *Biometals*, **16**, 403 (2003).
[45] R.A. Haque, N. Hasanudin, M.A. Iqbal, A. Ahmad, S. Hashim, A.M.S. Abdul Majid, M.B.K. Ahamed. *J. Coord. Chem.*, **66**, 3211 (2013).
[46] M.A. Iqbal, R.A. Haque, M.B.K. Ahamed, A.M.S. Abdul Majid, S.S. Al-Rawi. *Med. Chem. Res.*, **22**, 2455 (2013).
[47] K.M. Hindi, M.J. Panzner, C.A. Tessier, C.L. Cannon, W.J. Youngs. *Chem. Rev.*, **109**, 3859 (2009).
[48] J. Pernak, P. Chwała. *Eur. J. Med. Chem.*, **38**, 1035 (2003).
[49] J.W. Searl, R.C. Smith, S. Wyard. *J. Proc. Phys. Soc.*, **78**, 1174 (1961).
[50] C. Walsh. *Antibiotics*, ASM Press, Washington, DC (2003).
[51] K. Yamamoto, S. Kawanishi. *J. Biol. Chem.*, **264**, 15435 (1989).
[52] I.P. Dominique, M.J. Belousoff, L.B.G. Spiccia. *Coord. Chem. Rev.*, **256**, 897 (2012).